SIAM J. APPL. MATH.
Vol. 84, No. 1, pp. 114–138

TIPPING POINTS IN SEED DISPERSAL MUTUALISM DRIVEN BY ENVIRONMENTAL STOCHASTICITY*

TAO FENG†, ZHIPENG QIU‡, AND HAO WANG§

Abstract. The mechanism of seed dispersal mutualism is fundamental to understanding vegetation diversity and its conservation. In this study, we propose a stochastic model that extends the classical framework of seed dispersal mutualism to explore the effects of environmental stochasticity on mutualistic interactions between seed dispersers and plants. We first provide a comprehensive picture of the long-term dynamics of seed dispersal mutualism in deterministic and stochastic environments. We then analyze the relationship between stochasticity and the probability and time that seed dispersal mutualism tips between stable states. Additionally, we evaluate the extinction risk of seed dispersal mutualism for different population values and accordingly assign extinction warning levels to these values. The analysis reveals that the impact of environmental stochasticity on tipping phenomena is scenario-dependent but follows some interpretable trends. The probability (resp., time) of tipping towards the extinction state typically increases (resp., decreases) monotonically with noise intensity, while the probability of tipping towards the coexistence state typically peaks at intermediate noise intensity. Noise in animal populations contributes to tipping toward the coexistence state, whereas noise in plant populations slows down the tipping toward the coexistence state. Noise-induced changes in warning levels of initial population values are most pronounced near the boundaries of the basin of attraction, but sufficiently loud noise (especially for plant populations) may alter the risk far from these boundaries. These findings provide a theoretical explanation for the effect of environmental stochasticity on multistability transitions in seed dispersal mutualism and can be utilized to study the interplay between other population systems and environmental stochasticity.

Key words. seed dispersal mutualisms, environmental stochasticity, tipping point, coexistence, early warning

MSC codes. 34F05, 92B05

DOI. 10.1137/22M1531579

1. Introduction.

Seed dispersal mutualism is the backbone of ensuring the biodiversity and productivity of terrestrial habitats. It has been reported that about 56% of plant species worldwide rely on seed dispersers for reproduction [2, 44]. Seed dispersal mutualism is typically characterized by close cooperation between plant and animal species. During foraging, animals occasionally visit plants and receive

*Received by the editors October 31, 2022; accepted for publication (in revised form) November 6, 2023; published electronically January 30, 2024.
https://doi.org/10.1137/22M1531579

Funding: The first author's research was partially supported by the Natural Science Foundation of Jiangsu Province, People's Republic of China (grant BK20220553), the National Natural Science Foundation of China (grant 12201548), and the Scholarship Foundation of China Scholarship Council (grant 202308320279). The second author's research was partially funded by the National Natural Science Foundation of China (award 12071217). The third author's research was partially supported by the Natural Sciences and Engineering Research Council of Canada (Individual Discovery Grant RGPIN-2020-03911 and Discovery Accelerator Supplement Award RGPAS-2020-00090) and the Canada Research Chairs program (Tier 1 Canada Research Chair Award).

†School of Mathematical Science, Yangzhou University, Yangzhou, 225002, People's Republic of China (taofeng@yzu.edu.cn).

‡Interdisciplinary Center for Fundamental and Frontier Sciences, Nanjing University of Science and Technology, Jiangyin, 214443, People's Republic of China, and Department of Mathematics, Nanjing University of Science and Technology, Nanjing, 210094, People's Republic of China (nustqzp@njust.edu.cn).

§Corresponding author. Department of Mathematical and Statistical Sciences, University of Alberta, Edmonton, AB T6G 2G1, Canada (hao8@ualberta.ca).

nutritional rewards (such as nectar and fruit). In return, animals provide shelter and migration opportunities for plant seeds [10]. In recent years, seed dispersers have faced unprecedented threats from climate change, pesticides, and many other environmental factors [7, 47]. For example, climate change could potentially impact the range and migratory behavior of animals, consequently affecting their ability to distribute seeds [43]. Additionally, climate change can alter the traits of seeds, including their size, shape, and color, which could affect their attractiveness and adaptability to animal dispersers [31, 39]. Pesticides can adversely affect animal behavior, reproduction, and immune function, ultimately impacting seed dispersal behavior. Evidence suggests that organochlorine insecticides can reduce the energy reserves of bats and affect their reproductive abilities [34]. While there is evidence that environmental factors are responsible for the decline in seed dispersers, scientists still face challenges in understanding how these declines affect the dynamics of seed dispersal mutualisms.

Mathematical modeling frameworks provide an adequate opportunity to study the theoretical mechanisms of mutualism systems. Early theoretical studies of mutualism systems were based more on Lotka–Volterra differential equation models, representing mutualism systems as active feedback between species [20, 33]. For instance, Gause and Witt [16] provided a definite idea of the continuous passage from mutual depression to commensalism and symbiosis of species. Vandermeer and Boucher [46] pointed out that traditional neighborhood stability analysis for Lotka–Volterra mutualism does not accurately predict expected biological outcomes. It is necessary to modify the Lotka–Volterra model to provide nonlinear isoclines to achieve a minimum level of biological realism. By constructing a simple plant-animal symbiosis model, Bascompte, Jordano, and Olesen [3] demonstrated that the inherent asymmetry in coevolutionary networks might enhance long-term coexistence and promote the maintenance of biodiversity. Recent work on the dynamics of mutualism systems has favored consumer-resource models, which are characterized by advantages in discovering important dynamics such as the Allee effects and alternative states [19, 23, 36]. By integrating some fundamental characteristics of pollination ecology, Valdovinos et al. [45] proposed a novel consumer-resource model for plant-pollinator interactions. They found that pollination networks can maintain stability and diversity through the adaptive foraging of generalist pollinators. Johnson and Amarasekare [27] formulated mathematical models to explore whether obligatory reciprocity can persist solely through competition for benefits. They found that competition for benefits provides a biologically plausible mechanism for the long-term persistence of reciprocity and the assembly of complex community modules from initial pairwise interactions. They also emphasized that studying the impact of environmental stochasticity on driving species abundances below their extinction thresholds is an important future direction.

Environmental stochasticity refers to the unpredictable spatial and temporal fluctuations in environmental conditions [12]. Climate changes that belong to environmental stochasticity include natural fluctuations in temperature and precipitation patterns and extreme weather events such as droughts, heat waves, storms, and floods. Human-induced climate changes, such as greenhouse gas emissions and deforestation, can exacerbate environmental stochasticity by leading to more frequent and intense fluctuations in temperature and precipitation patterns. Pesticides can also be seen as a form of environmental stochasticity, as they introduce unpredictable and variable changes to the environment that can affect ecological processes and population dynamics. The ecological effects of environmental stochasticity were noted as early as 1898 but received much less attention [6]. Lee and Strauss [29] suggested that no environment is constant over time, and environmental stochasticity should always be included in population models. To be successful, plant-animal interactions in seed

dispersal mutualism must adapt to environmental changes. Therefore, the degree of stochasticity in the environment can significantly impact the dynamics of seed dispersal mutualism. Zhou et al. [47] pointed out that although the dynamics of seed dispersal mutualism are partly driven by deterministic intrinsic interactions (e.g., the relativity of returns), such mutualism relationships are particularly susceptible to stochastic extrinsic perturbations. Essentially, environmental stochasticity is unsuitable for statistical inference applications, which require large sample sizes. Thus, the effect of environmental stochasticity on the dynamics of seed dispersal mutualism is neither well documented nor well understood.

Multistability is a prevalent phenomenon in biological systems, which is characterized by the existence of several stable states that can be attained and maintained under the same external conditions [37]. When a system exhibits multiple stable states, minor changes may occur without significantly altering the state. However, once a tipping point is reached, the system undergoes irreversible changes, transitioning from one stable state to another [1]. Understanding the stable states and their transitions is crucial for comprehending the response mechanisms and stability of seed dispersal mutualisms, as these often involve interactions among multiple populations [28]. For instance, we can implement corresponding management measures to prevent irreversible situations by predicting an alternative stable state that seed dispersal mutualisms may enter when they experience disruption or disturbance. Furthermore, multiple stable states provide an opportunity to restore fragile seed dispersal mutualisms, as they can transition from one stable state to another, thereby re-establishing stable ecological conditions.

There is a growing awareness that environmental stochasticity can lead to tipping points in which an abrupt shift from a steady state to an alternate dynamic regime occurs [5, 9, 13]. For instance, large-scale bleaching events on the Great Barrier Reef in 2016 and 2017, caused by warm water anomalies, pushed the coral reefs beyond their tipping point, resulting in a shift from a coral-dominated to an algae-dominated ecosystem [24]. Post et al. [35] indicated that changes in temperature and precipitation patterns can cause a tipping point in Arctic tundra ecosystems, leading to rapid and irreversible changes in the vegetation and animal communities. In addition, tipping points have also been found in ecological cases such as grasslands [40], forests [41], and fish populations [42]. As tipping points can lead to the collapse of important ecological functions and are often closely linked with warning signals prior to these collapses, it is crucial to understand the mechanisms of tipping points for population conservation [8, 26]. To date, theoretical research on how environmental stochasticity affects tipping points has yielded many significant advances. For instance, Meng, Lai, and Grebogi [32] explored the effect of environmental stochasticity on average transient time in complex mutualistic networks of plant and pollinator species. Ryashko [38] analyzed how stochasticity contributes to tipping phenomena in the Higgins glycolysis model. However, few works have investigated the relationship between environmental stochasticity and the probability and time of a tipping point occurrence, as well as the problem of warning levels in seed dispersal mutualism, which will be the main focus of this paper.

The rest of this paper is organized as follows. Section 2 provides descriptions of deterministic and stochastic models. In section 3, we first study the global dynamics of the deterministic model in conjunction with the geometrical location of equilibria. Then we explore the long-term dynamics of the stochastic model, including the existence and uniqueness of global positive solutions, stochastic uniform boundedness, stochastic persistence, and extinction. The transient dynamics of the seed dispersal

mutualism in stochastic environments are presented in section 4, including confidence ellipses, tipping probability and time, and early warning classification. Theoretical findings, biological implications, and future work are discussed in section 5.

2. Model description. A recent notable contribution to seed dispersal mutualism comes from the work of Hale, Maes, and Valdovinos [19], which proposed a consumer-resource framework for describing the dynamics of seed dispersal mutualism. The model is described as follows:

$$\begin{aligned} \frac{dP}{dt} &= P\left[b_P f\left(g+\gamma\frac{aA}{1+ahP+aA}\right)-s_P P-d_P\right], \\ \frac{dA}{dt} &= A\left[b_A+\epsilon\frac{aP}{1+ahP}-s_A A-d_A\right], \end{aligned} \tag{2.1}$$

where $P(t)$ and $A(t)$ represent the population densities of plants and animals at time t, b_P and b_A denote the birth rates of plant and animal populations, and d_P and d_A are the mortality rates of plant and animal populations, respectively. f and g $(0 \le f, g \le 1)$ represent the natural seed dispersal (due to wind, etc.) and the germination proportion, respectively. Since animal viscera provides a good germination environment for seeds, the germination rate of seeds increases during animal dispersal, which is represented by $\gamma(0 < \gamma \le 1-g)$. a and h are the per-plant attack rate and handling time on rewards. ϵ refers to the efficiency with which an animal converts food rewards into offspring. s_P and s_A describe the crowding effect of plant and animal populations, respectively. In model (2.1), we assume that animals feed on fruits rather than plants themselves and the consumption of animal populations on plant fruits will not reduce the mortality of plant population, and thus no predation term is included in model (2.1). All parameters are set to be nonnegative for biological significance.

By modeling payoff as a function of the foraging rate by animals for plant rewards, Hale, Maes, and Valdovinos [19] created a nonlinear relationship between plant and animal populations. Although Hale, Maes, and Valdovinos [19] captured many aspects of the dynamics of seed dispersal mutualism, including the discovery that seed dispersal mutualism is stable at high density but exhibits different dynamics at low density, further work is warranted. In short, the main findings of Hale, Maes, and Valdovinos [19] are based on numerical simulations, and it is meaningful to explore the generalizability of related results theoretically. Furthermore, Hale, Maes, and Valdovinos [19] do not assess the potential impact of environmental stochasticity on the dynamics of seed dispersal mutualism.

In this work, we explore how environmental stochasticity affects the dynamics of seed dispersal mutualism. Since environmental stochasticity such as climate and rainfall are time-independent random variables, they are usually described mathematically by standard independent Brownian motion. Following previous modeling work [15, 25], we assume that environmental stochasticity mainly affects mortality in plant and animal populations, and

$$d_P \to d_P - \sigma_1 \dot{B}_1(t), \quad d_A \to d_A - \sigma_2 \dot{B}_2(t),$$

where $B_i(t)$ is a standard Brownian motion with intensity $\sigma_i^2, i = 1, 2$, and $\dot{B}_i(t), i = 1, 2$, denotes the time derivative of the standard Brownian motion $B_i(t)$, also known as the Brownian motion derivative or the Wiener process. Throughout this paper, we assume that $B_1(t)$ and $B_2(t)$ are defined on the complete probability space $(\Omega, \mathcal{F}, \mathbb{P})$

with filtration $\{\mathcal{F}_t\}_{t\geq 0}$ satisfying the usual conditions, where Ω and $\mathbb{P}$ denote the sample space and probability measure, respectively. More generally, we can obtain the seed dispersal mutualism system under stochastic environments as follows:

$$\begin{aligned} dP &= P\left[b_P f\left(g+\gamma\frac{aA}{1+ahP+aA}\right)-s_P P-d_P\right]dt+\sigma_1 P dB_1(t),\\ dA &= A\left[b_A+\epsilon\frac{aP}{1+ahP}-s_A A-d_A\right]dt+\sigma_2 A dB_2(t). \end{aligned} \tag{2.2}$$

3. Model analysis. In this section, we provide the threshold conditions for the long-term dynamics of the deterministic model (2.1) and the stochastic model (2.2). For brevity, the detailed proofs of some theorems have been moved to the appendices.

3.1. Global dynamics of the deterministic case. Since model (2.1) maps the population dynamics of seed dispersal mutualism, we first show that model (2.1) is biologically well defined.

LEMMA 3.1. *Model* (2.1) *is positively invariant in* $\mathbb{R}^2_+ := [0,\infty)^2$, *and for any given initial value* $(P(0),A(0))\in\mathbb{R}^2_+$, *the solution* $(P(t),A(t))$ *will eventually be attracted to the compact set*

$$C=\left\{(P,A)\in\mathbb{R}^2_+ : 0\leq P\leq\frac{b_P f(g+\gamma)-d_P}{s_P},\ 0\leq A\leq\frac{b_A-d_A+\frac{\epsilon}{h}}{s_A}\right\}.$$

Remark. Lemma 3.1 states that the density of plant and animal populations is nonnegative and bounded due to limited natural resources.

THEOREM 3.2 (boundary dynamics). *Model* (2.1) *always has an extinction equilibrium* $E_0=(0,0)$. *In addition to* E_0, *if* $r_P=b_P fg-d_P>0$, *model* (2.1) *has a plant-only equilibrium* $E_{P0}=(\frac{r_P}{s_P},0)$; *and if* $r_A=b_A-d_A>0$, *model* (2.1) *has an animal-only equilibrium* $E_{0A}=(0,\frac{r_A}{s_A})$. *Threshold conditions for the boundary dynamics are summarized in Table* 1.

Remark. Theorem 3.2 indicates that the boundary dynamics of the seed dispersal mutualism are closely related to the relationship between plant and animal populations. In detail, we have the following: (i) If the animal A and the plant P populations are mutually obligated (i.e., $r_P, r_A<0$), they may go extinct together. Otherwise, if at least one of them is a facultative mutualist of the other (i.e., $r_P>0$ or $r_A>0$), the two will not go extinct together. (ii) Suppose that the plant population is a facultative mutualist of the animal population. If the animal population is an obligate mutualist of the plant population, and the mortality rate of the animal population is much higher than the birth rate (i.e., $r_A<-\frac{\epsilon a r_P}{s_P+ahr_P}$), then the animal population will become extinct and the plant population will survive. Conversely, if $r_A>-\frac{\epsilon a r_P}{s_P+ahr_P}$, the plant population will not be able to survive alone in the event of

TABLE 1
Boundary dynamics of the deterministic model (2.1).

Equilibrium	Existence condition	Stability condition
$E_0=(0,0)$	Always	Sink point if $r_P<0$ and $r_A<0$, saddle point if $r_P>0$ or $r_A>0$
$E_{P0}=(\frac{r_P}{s_P},0)$	$r_P>0$	Sink point if $r_A<-\frac{\epsilon a r_P}{s_P+ahr_P}$, saddle point if $r_A>-\frac{\epsilon a r_P}{s_P+ahr_P}$
$E_{0A}=(0,\frac{r_A}{s_A})$	$r_A>0$	Sink point if $r_P<-\frac{b_P f\gamma a r_A}{s_A+ar_A}$, saddle point if $r_P>-\frac{b_P f\gamma a r_A}{s_A+ar_A}$

animal population extinction. (iii) Suppose that the animal population is a facultative mutualist of the plant population. If the plant population is an obligate mutualist of the animal population, and the mortality rate of the plant population is much higher than the birth rate (i.e., $r_P < -\frac{b_P f\gamma a r_A}{s_A + a r_A}$), then the plant population will become extinct and the animal population will survive. Otherwise, if $r_P > -\frac{b_P f\gamma a r_A}{s_A + a r_A}$, then the animal population will not be able to survive alone in the event of plant population extinction.

Next, we analyze the coexistence dynamics of model (2.1). Since the coexistence equilibria of model (2.1) are determined by a complex cubic equation that is mathematically difficult to solve, we aim to provide an intuitive method to capture the stability of coexisting equilibria without knowing their expressions.

THEOREM 3.3 (coexistence dynamics). *If $s_A r_P + r_P r_A a + r_A b_P f\gamma a > 0$, model* (2.1) *can have up to three coexistence equilibria. Otherwise, if $s_A r_P + r_P r_A a + r_A b_P f\gamma a < 0$, model* (2.1) *has at most two coexistence equilibria. Moreover, the stability of a coexistence equilibrium (when it exists) is determined by its geometric position in phase space:*

(i) *If model* (2.1) *has a unique coexistence equilibrium $E_1^* = (P_1^*, A_1^*)$, then $E_1^* = (P_1^*, A_1^*)$ is locally asymptotically stable.*

(ii) *If model* (2.1) *has two coexistence equilibria $E_i^* = (P_i^*, A_i^*)$, $i = 1, 2$, with $P_1^* < P_2^*$, then $E_1^* = (P_1^*, A_1^*)$ is unstable, and $E_2^* = (P_2^*, A_2^*)$ is locally asymptotically stable.*

(iii) *If model* (2.1) *has three coexistence equilibria $E_i^* = (P_i^*, A_i^*)$, $i = 1, 2, 3$, with $P_1^* < P_2^* < P_3^*$, then $E_1^* = (P_1^*, A_1^*)$ and $E_3^* = (P_1^*, A_1^*)$ are locally asymptotically stable, and $E_2^* = (P_2^*, A_2^*)$ is unstable.*

Remark. Theorem 3.3 indicates that the local stability of coexistence equilibria depends entirely on their geometric locations in phase space (i.e., the density of plant or animal populations). If there is a unique coexistence equilibrium, then the equilibrium is stable. If there are two coexistence equilibria, the one with high population density is stable and the other is unstable. If there are three coexistence equilibria, the coexistence equilibria with high or low population density are stable. In contrast, the one with intermediate population density is unstable. These theoretical results are consistent with the findings of Hale, Maes, and Valdovinos [19].

THEOREM 3.4 (global dynamics). *For any given initial value $(P(0), A(0)) \in \mathbb{R}_+^2$, the solutions of system* (2.1) *converge to those equilibria that are locally asymptotically stable, except for the solutions on stable manifolds of unstable equilibria.*

Proof. Let (ψ_1, ψ_2) be the vector field defined by system (2.1), and define the Dulac function as $B(P, A) = \frac{1}{PA}$. It follows that

$$\begin{aligned}\frac{\partial B\psi_1}{\partial P} + \frac{\partial B\psi_2}{\partial A} &= \frac{\partial}{\partial P}\left\{B(P,A)\left[b_P f\left(g + \gamma\frac{aA}{1+ahP+aA}\right) - s_P P - d_P\right]P\right\} \\ &\quad + \frac{\partial}{\partial A}\left\{B(P,A)\left[b_A + \epsilon\frac{aP}{1+ahP} - s_A A - d_A\right]A\right\} \\ &= -\frac{b_P f\gamma a^2 h}{(1+ahP+aA)^2} - \frac{s_P}{A} - \frac{s_A}{P} < 0.\end{aligned}$$

Therefore, by the Dulac criterion [18] we know that any trajectory of the system (2.1) starting with a nonnegative initial condition converges to a fixed point. ∎

Remark. Theorem 3.4 implies that any solution of the system (2.1) starting in $(P(0), A(0)) \in \mathbb{R}_+^2$ converges towards either a boundary equilibrium or a coexistence

equilibrium; i.e., the population sizes of plants and animals always stabilize to constant levels. In particular, if there is a unique stable equilibrium in system (2.1), the equilibrium is globally asymptotically stable. If there are multiple locally stable equilibria in model (2.1), then there is bistability or multistability between these equilibria.

3.2. Long-term dynamics of the stochastic case. Next, we study the long-term dynamics of the stochastic system (2.2). To study the existence and uniqueness of the global positive solution, we first verify the existence and uniqueness of the local positive solution and then show that the explosion time of the solution is infinite (see the existence-and-uniqueness theorem in Gray et al. [17]). The proof of stochastic uniform boundedness largely depends on the construction of suitable Lyapunov functions. Since the system (2.2) is a stochastic Kolmogorov system, we use the Lyapunov exponents method (see Theorems 1.1 and 1.3 in Hening and Nguyen [21]) to prove the stochastic persistence and extinction.

THEOREM 3.5 (existence and uniqueness of global positive solution). *For any initial value* $(P(0), A(0)) \in \mathbb{R}^2_+$*, there is a unique positive solution* $(P(t), A(t)) \in \mathbb{R}^2_+$ *of model* (2.2) *on* $t \geq 0$ *with probability one.*

Remark. Since P and A represent the densities of plant and animal populations, they should remain nonnegative. Theorem 3.5 suggests that the stochastic model (2.2) always has a unique nonnegative solution, i.e., the stochastic model (2.2) is biologically reasonable.

THEOREM 3.6 (stochastically ultimately bounded). *System* (2.2) *is stochastically ultimately bounded; i.e., for any* $\varepsilon \in (0,1)$*, there exists a positive constant* $\delta = \delta(\varepsilon)$ *such that for any given initial value* $(P(0), A(0)) \in \mathbb{R}^2_+$*, we have*

$$\limsup_{t \to +\infty} \mathbb{P}\{|(P(t), A(t))| > \delta\} \leq \varepsilon. \tag{3.1}$$

Remark. Stochastic ultimate boundedness is an important property of stochastic biological systems, which suggests that the solution will be ultimately bounded with a large probability. Theorem 3.6 indicates that the stochastic ultimate boundedness of the system (2.2) is robust to environmental stochasticity.

To study the stochastic persistence and extinction of model (2.2), we define the critical parameters

$$\begin{aligned} &\lambda_1(\delta^*) = r_P - \frac{1}{2}\sigma_1^2, \lambda_2(\delta^*) = r_A - \frac{1}{2}\sigma_2^2, \\ &\lambda_1(\mu_2) = \lambda_1(\delta^*) + b_P f \gamma a \int_{\mathbb{R}^o_{2+}} \frac{x_2}{1 + a x_2} \mu_2(d\mathbf{x}), \\ &\lambda_2(\mu_1) = \lambda_2(\delta^*) + \epsilon a \int_{\mathbb{R}^o_{1+}} \frac{x_1}{1 + a h x_1} \mu_1(d\mathbf{x}), \end{aligned} \tag{3.2}$$

where δ^* is the Dirac measure concentrated on 0, and $\mu_1(\cdot)$ and $\mu_2(\cdot)$ are respectively the probability measures with densities

$$\begin{aligned} p_1(x) &= \sqrt{\frac{2 s_P}{\pi}} \exp\left[-\frac{s_P}{\sigma_1^2} x^2 + \frac{2(b_P f g - d_P)x}{\sigma_1^2} + \frac{(b_P f g - d_P)^2}{2 s_P} - \frac{2}{\sigma_1^2} \right], \\ p_2(x) &= \sqrt{\frac{2 s_A}{\pi}} \exp\left[-\frac{s_A}{\sigma_2^2} x^2 + \frac{2(b_A - d_A)x}{\sigma_2^2} + \frac{(b_A - d_A)^2}{2 s_A} - \frac{2}{\sigma_2^2} \right], \end{aligned}$$

defined on $\mathbb{R}^o_{1,+} := \{(x_1, 0) : x_1 > 0\}$ and $\mathbb{R}^o_{2,+} := \{(0, x_2) : x_2 > 0\}$, respectively. The long-term dynamics of the stochastic model (2.2) are summarized as follows.

THEOREM 3.7 (stochastic persistence and extinction).

1. *If $\lambda_i(\delta^*) > 0, i = 1, 2$, then there exists a unique invariant probability measure π^* on $\mathbb{R}^{2,o}_+ := (0, \infty)^2$, and the transition probability $\mathbf{P}(t, x, \cdot) \in \mathbb{R}^{2,o}_+$ of $(P(t), A(t))$ converges to π^* in total variation exponentially fast.*
2. *If $\lambda_1(\delta^*) > 0$, $\lambda_2(\delta^*) < 0 < \lambda_2(\mu_1)$, then there exists a unique invariant probability measure π^* on $\mathbb{R}^{2,o}_+$, and the transition probability $\mathbf{P}(t, x, \cdot) \in \mathbb{R}^{2,o}_+$ of $(P(t), A(t))$ converges to π^* in total variation exponentially fast.*
3. *If $\lambda_2(\delta^*) > 0, \lambda_1(\delta^*) < 0 < \lambda_1(\mu_2)$, then there exists a unique invariant probability measure π^* on $\mathbb{R}^{2,o}_+$, and the transition probability $\mathbf{P}(t, x, \cdot) \in \mathbb{R}^{2,o}_+$ of $(P(t), A(t))$ converges to π^* in total variation exponentially fast.*
4. *If $\lambda_i(\delta^*) < 0, i = 1, 2$, then $P(t)$ and $A(t)$ converge to 0 at the exponential rate $\lambda_i(\delta^*)$, $i = 1, 2$, respectively.*
5. *If $\lambda_1(\delta^*) > 0$ and $\lambda_2(\mu_1) < 0$, then $A(t)$ converges to 0 at the exponential rate $\lambda_2(\mu_1)$, and the randomized occupation measure converges weakly to μ_1.*
6. *If $\lambda_2(\delta^*) > 0$ and $\lambda_1(\mu_2) < 0$, then $P(t)$ converges to 0 at the exponential rate $\lambda_1(\mu_2)$, and the randomized occupation measure converges weakly to μ_2.*

Proof. It is easy to verify that the solution of model (2.1) is nondegenerate diffusion and the per-capita growth rates of both populations are local Lipschitz functions. By direct calculation, we can get that

(3.3)

$$\begin{aligned}
h_1(P,A) + h_2(P,A) &\le P\left[b_P f(g+\gamma) - s_P P\right] + A\left[b_A + \frac{\epsilon}{h} - s_A A\right] \\
&\le \max\left\{b_P f(g+\gamma), b_A + \frac{\epsilon}{h}\right\}(P+A) - \min\{s_P, s_A\}(P^2 + A^2) \\
&\le \max\left\{b_P f(g+\gamma), b_A + \frac{\epsilon}{h}\right\}(P+A) - \frac{1}{2}\min\{s_P, s_A\}(P^2 + A^2) \\
&\quad - \min\{s_P, s_A\} PA \\
&\le \max\left\{b_P f(g+\gamma), b_A + \frac{\epsilon}{h}\right\}(P+A) - \frac{1}{2}\min\{s_P, s_A\}(1+P+A)^2 \\
&\quad + \frac{1}{2}\min\{s_P, s_A\} + \min\{s_P, s_A\}(P+A) \\
&\le \left\{\max\left\{b_P f(g+\gamma), b_A + \frac{\epsilon}{h}\right\} + \min\{s_P, s_A\}\right\}(1+P+A) \\
&\quad - \frac{1}{2}\min\{s_P, s_A\}(1+P+A)^2.
\end{aligned}$$

Therefore, one can choose $\gamma_b > 0$ small enough such that

(3.4)

$$\begin{aligned}
&\limsup_{P+A\to+\infty}\left[\frac{h_1(P,A) + h_2(P,A)}{1+P+A} + \gamma_b\left(1 + \frac{|h_1(P,A)|}{P} + \frac{|h_2(P,A)|}{A} + \sum_{i=1}^{2}\sigma_i^2\right)\right. \\
&\quad \left. - \frac{1}{2}\frac{(\sigma_1 P + \sigma_2 A)^2}{(1+P+A)^2}\right] \\
&\le \limsup_{P+A\to+\infty}\left[-\left[\frac{1}{2}\min\{s_P, s_A\} - \gamma_b \max\{s_P, s_A\}\right](P+A)\right] + \gamma_b\left(1 + \sum_{i=1}^{2}\sigma_i^2\right) \\
&\quad + \gamma_b\left\{b_P f(g+\gamma) + b_A + \frac{\epsilon}{h}\right\} + \left\{\max\left\{b_P f(g+\gamma), b_A + \frac{\epsilon}{h}\right\} + \min\{s_P, s_A\}\right\} \\
&< 0,
\end{aligned}$$

which indicates that the stochastic model (2.2) has a unique strong solution and that the family of transition probabilities for this solution is tight.

Similarly, we can choose $\delta_1 \in (0,1)$ sufficiently small such that

$$\begin{aligned}(3.5)\qquad &\lim_{P+A\to+\infty} \frac{(P+A)^{\delta_1}\sum_{i=1,2}\sigma_i^2}{1+\sum_{i=1,2}\sigma_i^2+\frac{|h_1(P,A)|}{P}+\frac{|h_2(P,A)|}{A}}\\ &\le \lim_{P+A\to+\infty}\frac{(P+A)^{\delta_1}\sum_{i=1,2}\sigma_i^2}{1+\sum_{i=1,2}\sigma_i^2+\min\{s_P,s_A\}(P+A)}=0.\end{aligned}$$

Thus, the growth rate of the diffusion part is slightly lower than that of the drift part.

In view of Theorem 1.1 in Hening and Nguyen [21], we have

$$\lambda_1(\delta^*)=b_P f g-d_P-\frac{1}{2}\sigma_1^2,\ \lambda_2(\delta^*)=b_A-d_A-\frac{1}{2}\sigma_2^2,$$

where δ^* is a Dirac measure concentrated on 0. The following hold: (i) If $\lambda_1(\delta^*)<0$, there is no invariant probability measure on $\mathbb{R}^o_{1,+}:=\{(x_1,0):x_1>0\}$; otherwise, if $\lambda_1(\delta^*)>0$, there is a unique invariant probability measure μ_1 on $\mathbb{R}^o_{1,+}$. (ii) If $\lambda_2(\delta^*)<0$, there is no invariant probability measure on $\mathbb{R}^o_{2,+}:=\{(0,x_2):x_2>0\}$; otherwise, if $\lambda_2(\delta^*)>0$, there is a unique invariant probability measure μ_2 on $\mathbb{R}^o_{2,+}$.

Define

$$\begin{aligned}(3.6)\qquad \lambda_1(\mu_2)&=\int_{\mathbb{R}^o_{2,+}}\left[b_P f g-d_P-\frac{1}{2}\sigma_1^2+b_P f\gamma\frac{ax_2}{1+ax_2}\right]\mu_2(d\mathbf{x}),\\ \lambda_2(\mu_1)&=\int_{\mathbb{R}^o_{1,+}}\left[b_A-d_A-\frac{1}{2}\sigma_2^2+\epsilon a\frac{ax_1}{1+ahx_1}\right]\mu_1(d\mathbf{x}).\end{aligned}$$

Solving the Fokker–Plank equation

$$\begin{aligned}(3.7)\qquad 0&=-\frac{d}{dx}[p_1(x)(b_P f g-s_P x-d_P)]+\frac{d^2}{dx^2}\left(\frac{1}{2}\sigma_1^2 p_1(x)\right),\\ 0&=-\frac{d}{dx}[p_2(x)(b_A-s_A x-d_A)]+\frac{d^2}{dx^2}\left(\frac{1}{2}\sigma_2^2 p_2(x)\right),\end{aligned}$$

we obtain the density $p_i(\cdot)$ of the invariant probability measure μ_i, $i=1,2$, as follows:

$$\begin{aligned}(3.8)\qquad p_1(x)&=\sqrt{\frac{2s_P}{\pi}}\exp\left[-\frac{s_P}{\sigma_1^2}x^2+\frac{2(b_P f g-d_P)x}{\sigma_1^2}+\frac{(b_P f g-d_P)^2}{2s_P}-\frac{2}{\sigma_1^2}\right],\\ p_2(x)&=\sqrt{\frac{2s_A}{\pi}}\exp\left[-\frac{s_A}{\sigma_2^2}x^2+\frac{2(b_A-d_A)x}{\sigma_2^2}+\frac{(b_A-d_A)^2}{2s_A}-\frac{2}{\sigma_2^2}\right].\end{aligned}$$

The remainder of proof can be directly obtained by Theorems 1.1 and 1.3 in Hening and Nguyen [21] and is therefore omitted. ∎

Remark. Theorem 3.7 provides threshold conditions for the survival of plant and animal populations in stochastic environments: (i) If the intensity of environmental stochasticity from the plant (resp., animal) population is weak enough, the plant (resp., animal) population is strongly stochastically persistent. In this case, the system has a unique invariant probability measure π^* on $\mathbb{R}^{2,o}_+$, indicating that the seed dispersal mutualism does not change its statistical characteristics (i.e., the mean and variance) over time, and the seed dispersal mutualism has the same behavior averaged over time as averaged over the probability space. This feature provides

great convenience for further exploring the effect of environmental stochasticity on dispersal mutualism numerically: the distribution of seed dispersal mutualism can be estimated by simulating a sample trajectory of the stochastic model (2.2). (ii) If the intensity of environmental stochasticity from the plant (resp., animal) population is strong enough, the plant (resp., animal) population will go extinct with probability 1. In particular, if the environmental stochasticity does not exist, Theorem 3.7 suggests that the plant (resp., animal) population will not go extinct as long as it is a facultative mutualism.

4. Noise-induced transient dynamics. In this section, we explore how environmental stochasticity affects the transient dynamics of seed dispersal mutualism by studying the noise-induced steady-state transition between extinction and coexistence states. First, confidence ellipses are constructed for different fiducial probabilities using the stochastic sensitivity function method (see Bashkirtseva, Ryazanova, and Ryashko [4]). Second, we analyze the relationship between stochasticity and the probability and time that seed dispersal mutualism tips between stable states. Finally, we customize a warning classification for the initial plant and animal population levels.

4.1. Noise-induced extinction via confidence ellipses. To explore the effect of environmental stochasticity on the extinction of the seed dispersal mutualism, we adapt the parameters of Hale, Maes, and Valdovinoset [19] as follows (the description and units are shown in Table 2): $b_P = 1$, $f = 1$, $g = 0.5, \gamma = 0.5$, $a = 0.85$, $h = 1$, $s_P = 0.05$, $d_P = 0.7$, $b_A = 1$, $\epsilon = 2$, $s_A = 0.15$, $d_A = 1.5$. By direct calculation, it can be seen that $r_P = b_P f g - d_P = -0.2$, $r_A = b_A - d_A = -0.5 < 0$, and the function $H_0(P)$ has two positive real roots $P_1^* = 0.708168$ and $P_2^* = 2.13781$. Therefore, the deterministic model (2.1) has a unique extinction equilibrium $E_0 = (0, 0)$ and two coexistence equilibria $E_1^* = (0.708168, 1.67677), E_2^* = (2.137808, 5.26706)$. From Theorems 3.2 and 3.3, we know that the deterministic model (2.1) exhibits bistability between the extinction equilibrium E_0 and the larger coexistence equilibrium E_2^*, while the smaller coexistence equilibrium E_1^* is unstable.

Figure 1(a) shows the phase diagram of the deterministic model (2.1), where the red dashed line represents the separatrix of the attraction basins between E_0 and E_2^*. In this case, any solution starting from the left side of the separatrix will eventually

TABLE 2

Parameter values for the seed dispersal mutualism. Except for the noise intensities σ_1 and σ_2, which are assumed, all other parameters are sourced from Hale, Maes, and Valdovinoset [19].

Parameter	Description	Default	Unit
b_P	Birth rate of plant population	1	t^{-1}
d_P	Mortality rate of plant population	0.7	t^{-1}
s_P	Crowding effect of plant population	0.05	P^{-2}
b_A	Birth rate of animal population	1	t^{-1}
d_A	Mortality rate of animal population	1.5	t^{-1}
s_A	Crowding effect of animal population	0.15	$A^{-2}t^{-1}$
a	Per-plant attack rate on rewards	0.85	$P^{-1}t^{-1}$
f	Natural seed dispersal proportion	1	Unitless
g	Natural germination proportion	0.5	Unitless
h	Per-plant handling time on rewards	1	t
ϵ	Efficiency of converting rewards into animal offspring	2	Unitless
γ	Germination rate of seeds increases during animal dispersal	0.5	Unitless
σ_1	Intensity of environmental stochasticity from plant population	0.05	Unitless
σ_2	Intensity of environmental stochasticity from animal population	0.05	Unitless

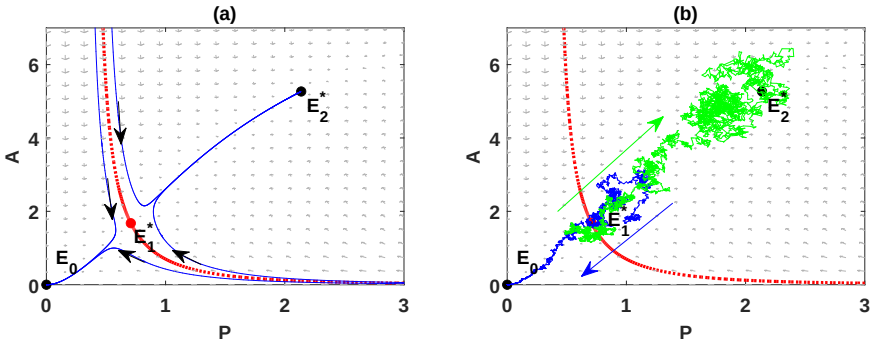

FIG. 1. *Pairwise phase diagrams of the deterministic model* (2.1) *and the stochastic model* (2.2). *The parameters are given by* $b_P = 1$, $f = 1$, $g = 0.5$, $\gamma = 0.5$, $a = 0.85$, $h = 1$, $s_P = 0.05$, $d_P = 0.7$, $b_A = 1$, $\epsilon = 2$, $s_A = 0.15$, $d_A = 1.5$. *In this case, the deterministic model* (2.1) *has a unique extinction equilibrium* E_0 *and two coexistence equilibria* E_1^*, E_2^*, *where* E_0 *and* E_2^* *are locally stable, and* E_1^* *is unstable. The red dotted lines denote the separatrix between the attraction basins of* E_0 *and* E_2^*. *In Figure* 1(b), *the noise intensities are given by* $\sigma_1 = 0.1$ *and* $\sigma_2 = 0.1$. *The blue curve shows that the solution starting from the basin of attraction of* E_2^* *may pass through the separatrix and stabilize to* E_0. *The green curve shows that the solution starting from the basin of attraction of* E_0 *may pass through the separatrix and finally reach the small neighborhood of* E_2^*.

converge to the extinction equilibrium E_0, and any solution starting from the right side of the separatrix will eventually converge to the coexistence equilibrium E_2^*. When the intensity of environmental stochasticity is sufficiently weak (an extreme scenario is a degradation to the deterministic model), the solution from one steady-state attraction basin will not cross the separatrix into another steady-state attraction basin (not shown here). As the intensity of environmental stochasticity increases, a solution starting from the attraction basin of E_0 gets a chance to pass through the separatrix to enter the small neighborhood of E_2^*, while a solution starting from the attraction basin of E_2^* may tip to the extinction state E_0 (see Figure 1(b)).

To determine the critical threshold of noise intensity that makes the solution transition from the coexistence state $E_2^* = (P_2^*, A_2^*)$ to the extinction state $E_0 = (0, 0)$, we employ the stochastic sensitivity function method proposed in Bashkirtseva, Ryazanova, and Ryashko [4]. For brevity, we consider only the case where the noise intensity is symmetric, i.e., $\sigma_1 = \sigma_2 = \sigma$. By direct calculation, the Jacobian matrix and diffusion matrix at the coexistence state $E_2^* = (P_2^*, A_2^*)$ can be expressed as

$$F = \begin{pmatrix} f_{11} & f_{12} \\ f_{21} & f_{22} \end{pmatrix}, \quad G = \begin{pmatrix} g_{11} & 0 \\ 0 & g_{22} \end{pmatrix},$$

where

$$f_{11} = -P_2^* \left[\frac{b_P f \gamma a^2 h A_2^*}{(1 + ahP_2^* + aA_2^*)^2} + s_P \right], \quad f_{12} = \frac{b_P f \gamma a P_2^* (1 + ahP_2^*)}{(1 + ahP_2^* + aA_2^*)^2},$$
$$f_{21} = \frac{\epsilon a A_2^*}{(1 + ahP_2^*)^2}, \quad f_{22} = -s_A A_2^*,$$

and

$$g_{11} = (P_2^*)^2, g_{22} = (A_2^*)^2.$$

Define the stochastic sensitivity matrix as

$$W = \begin{pmatrix} w_{11} & w_{12} \\ w_{21} & w_{22} \end{pmatrix}$$

and its transpose as W', i.e., $(W')' = W$. It follows that the stochastic sensitivity matrix should satisfy

$$FW + WF' = -G,$$

which can be expressed as

$$\begin{aligned} 2f_{11}w_{11} + f_{12}w_{12} + f_{12}w_{21} &= -g_{11}, \\ f_{21}w_{11} + (f_{11} + f_{22})w_{12} + f_{12}w_{22} &= 0, \\ f_{21}w_{11} + (f_{11} + f_{22})w_{21} + f_{12}w_{22} &= 0, \\ f_{21}w_{12} + f_{21}w_{21} + 2f_{22}w_{22} &= -g_{22}. \end{aligned}$$

By simple calculation, we can get that

$$W = \begin{pmatrix} 20.1813 & 29.3997 \\ 29.3997 & 121.604 \end{pmatrix}, \quad W^{-1} = \begin{pmatrix} 0.0765 & -0.0185 \\ -0.0185 & 0.0127 \end{pmatrix}.$$

Since the confidence ellipse equation around the coexistence equilibrium E_2^* is given by

$$\langle (P - P_2^*, A - A_2^*)', W^{-1}(P - P_2^*, A - A_2^*)' \rangle = 2\sigma^2 \log \frac{1}{1 - \mathcal{P}},$$

where $\mathcal{P}$ is the fiducial probability, it follows that the confidence ellipse equation can be shown as

$$\begin{aligned} 2\sigma^2 \log \frac{1}{1 - \mathcal{P}} = {} & 0.0765(P - 2.137808)^2 + 58.7994(P - 2.137808)(A - 5.26706) \\ & + 0.0127(A - 5.26706)^2. \end{aligned}$$

In Figure 2(a), the green line represents the confidence ellipse of E_2^* with noise intensity $\sigma_1 = \sigma_2 = 0.1$, the black solid point represents the phase of E_2^*, and the blue solid points represent the phase of the stochastic solution at $T = 2000$. Intuitively, most samples are distributed within the confidence ellipse, and only a few fall outside the confidence ellipse. In addition, few samples coincide with the extinction equilibrium E_0, which is evidence of solution switching from coexistence state E_2^* to extinction state E_0. Figure 2(b) shows that the confidence ellipse area is positively correlated with the intensity of environmental stochasticity. When the intensity of environmental stochasticity increases to about $\sigma = 0.14$, the confidence ellipse is tangent to the separatrix. Therefore, $\sigma = 0.14$ can be regarded as the critical threshold of noise intensity that makes the solution transition from the coexistence state $E_2^* = (P_2^*, A_2^*)$ to the extinction state $E_0 = (0, 0)$. If the noise intensity exceeds the critical threshold $\sigma = 0.14$, the transition probability is expected to increase substantially.

4.2. Tipping probability and time between steady states. In this subsection, we first give two critical definitions: tipping probability and tipping time. Then we study how environmental stochasticity relates to the probability and time of transition from one steady state to another.

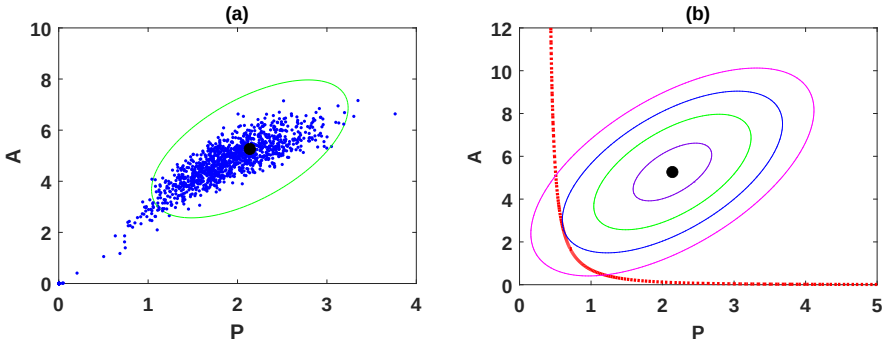

FIG. 2. (a) *Random states (2,000 samples, blue dots) and coexistence* E_2^* *(black dot) of the stochastic model* (2.2) *and confidence ellipse (green oval) for* $\sigma = 0.1$. (b) *Separatrix (red dotted line), coexistence* E_2^* *(black dot), and confidence ellipses for* $\sigma = 0.05$ *(purple oval),* $\sigma = 0.1$ *(green oval),* $\sigma = 0.14$ *(blue oval), and* $\sigma = 0.18$ *(pink oval).*

DEFINITION 4.1 (tipping probability and tipping time). *Consider the noise-induced system*

$$dX(t) = \mathbf{F}(X)dt + \sum_{m=1}^{k} \mathbf{G}_m(X)dB_m(t) \tag{4.1}$$

and the corresponding truncated system (i.e., with $\mathbf{G}_m(X) = 0$*), where* $\mathbf{F}, \mathbf{G_m} \in \mathbb{R}^n$*,* $B_m(t)$ *is a standard* n*-dimensional independent Brownian motion. Assume that the truncated system has* $n (n \geq 2)$ *steady states* $E_i, i = 1, 2, \ldots, n$ *(e.g., stable equilibria or stable cycles). When a solution starts from the basin of attraction of steady state* E_1*, we call the probability that the solution crosses the separatrix and settles within the basin of attraction of steady state* E_j *within a predetermined time interval* T *as the tipping probability of the solution from the steady state* E_i *to the steady state* E_j*. In addition, the time consumed by the whole tipping process is called a tipping time.*

It can be seen from subsection 4.1 that there is bistability between the extinction equilibrium E_0 and the larger coexistence equilibrium E_2^* in the truncated system (2.1). Therefore, we mainly focus on how environmental stochasticity affects the state transition between the extinction equilibrium E_0 and the coexistence equilibrium E_2^*. To proceed, we discretize the stochastic model (2.2) as

$$\begin{aligned} \phi_{k+1} = \phi_k + \mathbf{F}(\phi_k)\Delta t + \mathbf{G}(\phi_k)\xi_k\sqrt{(\Delta t)} \\ + \frac{1}{2}\sqrt{\Delta t}(\xi_k^2 - 1)(\mathbf{G}(\phi_k + \sqrt{\Delta t}g(\phi_k)) - \mathbf{G}(\phi_k)), \end{aligned} \tag{4.2}$$

where the time step Δt is small enough, ξ_k, $k = 1, 2$, obey the Gaussian distribution $N(0, 1)$, $\phi_k = (x(k), y(k))'$, $x = (x_1, x_2)' \in \mathbb{R}_+^2$, and the vector-valued functions $b, \sigma : \mathbb{R}_+^2 \to \mathbb{R}^2$ are given by

$$\mathbf{F}(x) = \begin{bmatrix} x_1\left[b_P f\left(g + \gamma\frac{ax_2}{1+ahx_1+ax_2}\right) - s_P x_1 - d_P\right] \\ x_2\left[b_A + \epsilon\frac{ax_2}{1+ahx_1} - s_A x_2 - d_A\right] \end{bmatrix}, \mathbf{G}(x) = \begin{bmatrix} \sigma_1 x_1 \\ \sigma_2 x_2 \end{bmatrix}.$$

With the help of MATLAB 2021a software and the Euler–Maruyama numerical algorithm [22], we run the discretized model (4.2) a total of 10,000 times and approximate

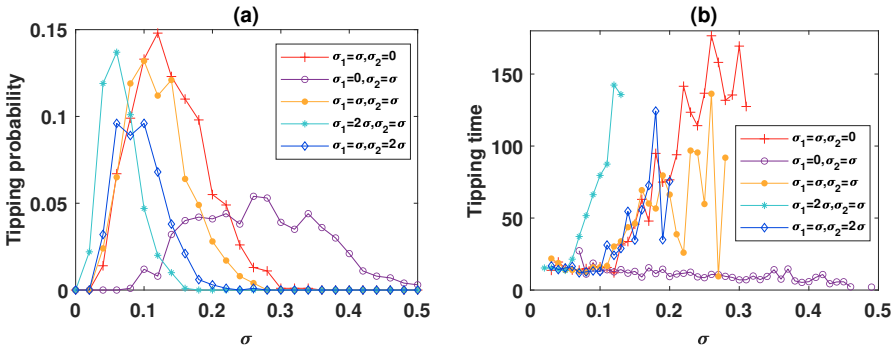

FIG. 3. *Tipping probability and tipping time from extinction state to coexistence state of the stochastic system* (2.2) *with parameters* $b_P = 1$, $f = 1$, $g = 0.5$, $\gamma = 0.5$, $a = 0.85$, $h = 1$, $s_P = 0.05$, $d_P = 0.7$, $b_A = 1$, $\epsilon = 2$, $s_A = 0.15$, $d_A = 1.5$, *and* $(P(0), A(0)) = (0.6, 1.6)$.

the tipping probability by estimating the frequency of steady-state switching in these samples. Similarly, the tipping time is estimated by calculating the average period of the tipping process over 10,000 samples.

When the system starts from the basin of attraction of E_0, we observe a nonmonotonic relationship between the tipping probability and the intensity of environmental stochasticity. Specifically, as the noise intensity increases, the tipping probability initially increases, reaches a peak, and then decreases, ultimately approaching zero (Figure 3(a)). The peak of tipping probability is influenced by the source of stochasticity: an increase in the noise intensity from the plant population leads to a higher peak, while noise from the animal population has the opposite effect. Furthermore, the tipping time is also affected by environmental stochasticity, showing a negative correlation with noise intensity when the stochasticity arises solely from the animal population and a positive correlation with noise intensity when the plant population is also subject to stochasticity (Figure 3(b)). These findings suggest that environmental stochasticity may ameliorate the unfavorable survival conditions that lead to extinction when seed dispersal mutualism is in danger of disappearing. In particular, stochasticity from the plant population seems to be more beneficial for the survival of seed dispersal mutualism than stochasticity from the animal population.

On the other hand, when the system departs from the basin of attraction of E_2^*, we observe a positive correlation between the tipping probability and the intensity of environmental stochasticity (Figure 4(a)). In this case, when the noise intensity is sufficiently large, the tipping phenomenon occurs with a probability of 1, and the tipping time is inversely proportional to the intensity of environmental stochasticity (see Figure 4(b)). These findings indicate that environmental stochasticity can disrupt the coexistence of seed dispersal mutualism and ultimately lead to its extinction. Moreover, an increase in the intensity of environmental stochasticity can accelerate the time to extinction of seed dispersal mutualism.

4.3. Safe area and early warning classification. Given the commonly observed relationship between tipping probability and population density in seed dispersal mutualism, we investigate the susceptibility of different population densities to undergo tipping from a coexistence steady state to an extinction steady state. We subsequently develop an early warning classification based on the tipping probability.

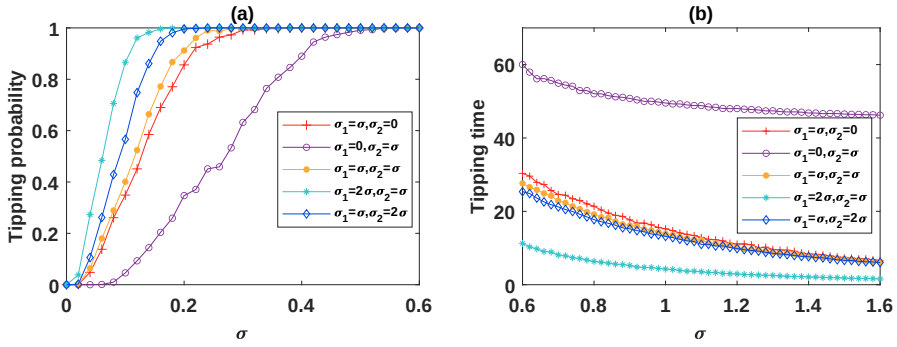

FIG. 4. *Tipping probability and tipping time from coexistence state to extinction state of the stochastic system* (2.2) *with parameters* $b_P = 1$, $f = 1$, $g = 0.5, \gamma = 0.5$, $a = 0.85$, $h = 1$, $s_P = 0.05$, $d_P = 0.7$, $b_A = 1$, $\epsilon = 2$, $s_A = 0.15$, $d_A = 1.5$, *and* $(P(0), A(0)) = (0.8, 2)$.

TABLE 3
Warning levels and associated extinction probabilities.

Warning level	Extinction probability	Marker color
Level-I warning (Red warning)	$\geq 80\%$	Red
Level-II warning (Orange warning)	50%-80%	Orange
Level-III warning (Yellow warning)	20%-50%	Yellow
Level-IV warning (Blue warning)	$\leq 20\%$	Blue

The early warning classification is characterized by four distinct levels: (i) Level-I warning, or red warning, indicates an extinction probability surpassing 80%; (ii) Level-II warning, or orange warning, denotes an extinction probability ranging between 50% and 80%; (iii) Level-III warning, or yellow warning, signifies an extinction probability between 20% and 50%; and (iv) Level-IV warning, or blue warning, corresponds to an extinction probability not exceeding 20% (see Table 3 for details).

In the absence of environmental stochasticity, the fate of seed dispersal mutualism is determined by the population density relative to the separatrix. If the population density is to the left of the separatrix, the seed dispersal mutualism will become extinct, and the corresponding area is identified as a red warning. Conversely, if the population density is to the right of the separatrix, the seed dispersal mutualism will persist, and the corresponding area is given a blue warning (Figure 5(a)).

However, when environmental stochasticity from the plant population is included, the warning levels on either side of the separatrix change. Specifically, some regions on the left side of the separatrix transition from the red warning to the orange warning, whereas some regions on the right side of the separatrix shift from the blue warning to the yellow warning (Figure 5(b)). These observations suggest that environmental stochasticity from the plant population has a diverse impact on seed dispersal mutualism, with the potential to contribute to the survival of seed dispersal mutualism when it is deterministically extinct or poses an extinction risk when it is deterministically persistent. In contrast, environmental stochasticity from the animal population has little impact on the seed dispersal mutualism, as evident from the minor changes in warning levels observed in a small neighborhood on either side of the separatrix (Figure 5(c)).

When the intensity of environmental stochasticity from plant and animal populations is symmetric, the resulting changes in the warning area are similar to those

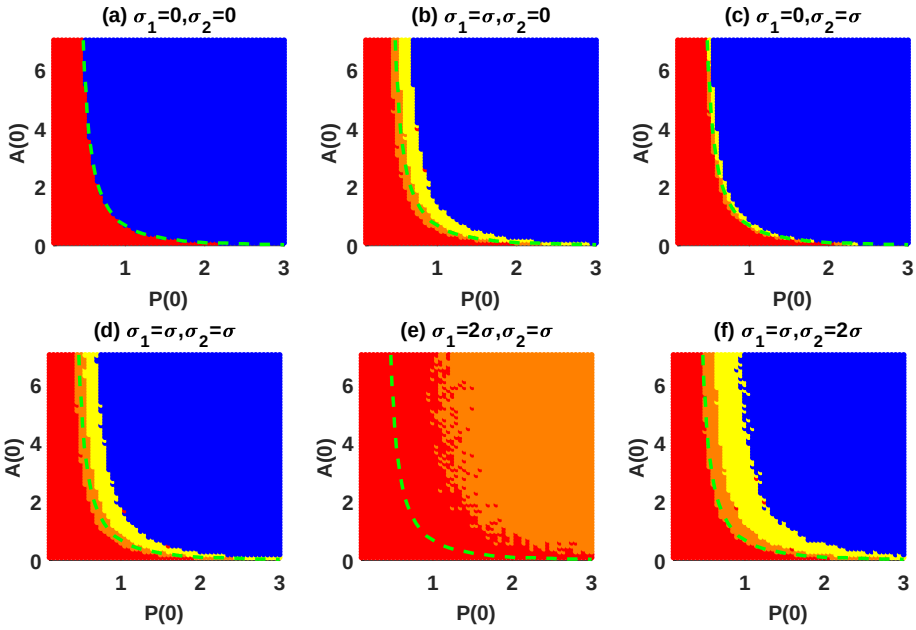

FIG. 5. *Warning level of the stochastic system* (2.2) *with parameters* $b_P = 1$, $f = 1$, $g = 0.5, \gamma = 0.5$, $a = 0.85$, $h = 1$, $s_P = 0.05$, $d_P = 0.7$, $b_A = 1$, $\epsilon = 2$, $s_A = 0.15$, $d_A = 1.5$, *and* $\sigma = 0.02$. *The blue, yellow, orange, and red areas indicate the probability of collapse of plant and animal populations as* 0%–20%, 20%–50%, 50%–80%, *and* 80%–100%, *respectively. The green line is the separatrix of the basins of attraction.*

observed when environmental stochasticity is only from the plant population (Figure 5(d)). However, when the environmental stochasticity from the plant population is twice as strong as that from the animal population, areas to the right of the separatrix are divided into a red warning zone and an orange warning zone (Figure 5(e)). Conversely, when the environmental stochasticity from the animal population is twice as strong as that from the plant population, the warning level changes occur in parts of the area to the right of the separatrix, resulting in an orange warning zone, a yellow warning zone, and a blue warning zone (Figure 5(f)). These observations demonstrate that environmental stochasticity from both plant and animal populations may contribute to the extinction of seed dispersal mutualism when it is deterministically persistent. Notably, when the intensities of environmental stochasticity from plant and animal populations are symmetric, the environmental stochasticity from the plant population dominates the warning classification.

5. Discussion. Seed dispersal mutualism is an indispensable type of symbiosis with irreplaceable value in maintaining the robustness and sustainable development of ecosystems. A recent study by Hale, Maes, and Valdovinos [19] developed a mathematical framework for studying seed dispersal mutualism, in which animals can improve seed germination rate by chewing or digesting fruits. Although their numerical simulations revealed bistability between coexistence and extinction states, the underlying mechanisms driving this behavior are not yet fully understood. Furthermore, the impact of environmental stochasticity on seed dispersal mutualism has not been thoroughly assessed.

This study examines the global dynamics of seed dispersal mutualism in deterministic environments. Our theoretical results show that the stability of the extinction state is contingent upon the nature of the mutualism. Specifically, if both plant and animal populations are obligately mutualistic, they will undergo extinction together. However, if the plant population is facultatively mutualistic while the animal population is obligately mutualistic, the plant population can persist independently if the animal population goes extinct, and vice versa. We also find that a coexistence state is stable if it is unique. If there are two coexisting states, the one with more animal and plant populations is stable, while the other is unstable. If three coexistence states exist, the one with a moderate density of plant and animal populations is unstable, while the other two are stable. These theoretical findings are supported by the observations of Hale, Maes, and Valdovinos [19].

We investigate the long-term dynamics of seed dispersal mutualism in stochastic settings. Our analysis identifies critical conditions for the stochastic persistence and extinction of plant and animal populations. Specifically, we find that if the intensity of environmental stochasticity surpasses a certain threshold, the populations will inevitably go extinct. Furthermore, we establish critical conditions for a unique invariant probability measure for the stochastic system. This indicates that the statistical properties, such as the mean and variance, of seed dispersal mutualism remain unchanged over time. In other words, the long-term behavior of seed dispersal mutualism is equivalent to its behavior averaged over the probability space. This property enables us to estimate the distribution of seed dispersal mutualism by simulating a sample trajectory of the stochastic model. To learn more about this property, we refer the reader to Mao [30] and Ellner and Rees [11].

We explore how environmental stochasticity affects the transient dynamics of seed dispersal mutualism. To achieve this, we employ the stochastic sensitivity function technique outlined in Bashkirtseva, Ryazanova, and Ryashko [4] to generate confidence ellipses for different fiducial probabilities. This approach allows us to identify a critical threshold of noise intensity necessary for a solution to transition from a coexistence state to an extinction state. If the noise intensity exceeds the critical threshold, we anticipate a significant increase in the transition probability. Moreover, we introduce two innovative concepts, tipping probability and tipping time, to gain deeper insight into how environmental stochasticity drives steady-state transitions in seed dispersal mutualism. These definitions describe the likelihood and duration required for steady-state transitions to occur. As tipping probability is typically linked to the population density of seed dispersal mutualism, we also explore which areas of the population density are more susceptible to tipping from the coexistence steady state to the extinction steady state. The numerical findings suggest that the influence of environmental stochasticity on seed dispersal mutualism is contingent on the particular circumstance. Specifically, environmental stochasticity may alleviate adverse survival conditions that precipitate extinction when seed dispersal mutualism is at risk of vanishing. Conversely, environmental stochasticity may also destabilize the coexistence of seed dispersal mutualism, ultimately resulting in its demise.

Despite our theoretical proposal positing the plausibility of three coexistence states in the seed dispersal mutualism, no parameters have been identified that corroborate this scenario (as confirmed by private communication with K. R. Hale). An intriguing avenue for future research would be to investigate how environmental stochasticity impacts the transition between coexistence steady states, provided that the parameters necessary for the existence of three coexistence equilibria are discovered. Additionally, future research will examine the combined influence of spatial

dispersal and environmental stochasticity on seed dispersal mutualism, focusing on synergistic effects. Expanding the overarching framework to specific biological processes, such as the mutualistic relationship between the social Azteca ants and the Cecropia trees, also represents a captivating area of inquiry [14].

Appendix A. Proof of Theorem 3.2.

Proof. Define

$$\begin{aligned} h_1(P,A) &= P\left[b_P f\left(g+\gamma\frac{aA}{1+ahP+aA}\right)-s_P P-d_P\right], \\ h_2(P,A) &= A\left[b_A+\epsilon\frac{aP}{1+ahP}-s_A A-d_A\right]. \end{aligned} \tag{A.1}$$

An equilibrium $E^*=(P^*,A^*)$ of model (2.1) should satisfy $h_i(P^*,A^*)=0, i=1,2$. Simple calculation shows that model (2.1) always has an extinction equilibrium $E_0=(0,0)$. If $r_P=b_P f g-d_P>0$, model (2.1) has a plant-only equilibrium E_{P0}, while if $r_A=b_A-d_A>0$, model (2.1) has an animal-only equilibrium E_{0A}.

In the following, we study the stability of these boundary equilibria:

(1) *Stability of the extinction equilibrium* E_0. Since the Jacobian matrix of model (2.1) evaluated at $E_0=(0,0)$ is given by

$$J(E_0)=\begin{pmatrix} r_P & 0 \\ 0 & r_A \end{pmatrix},$$

it follows that $\lambda_1=r_P$ and $\lambda_2=r_A$. That is, the extinction equilibrium E_0 is locally stable if $r_P, r_A<0$, while if $r_P>0$ or $r_A>0$, E_0 is unstable.

(2) *Stability of the plant-only equilibrium* E_{P0}. Evaluating the Jacobian matrix at E_{P0}, we obtain

$$J(E_{P0})=\begin{pmatrix} -r_P & \frac{b_P f\gamma a r_P}{s_P+ahr_P} \\ 0 & r_A+\frac{\epsilon a r_P}{s_P+ahr_P} \end{pmatrix}.$$

The corresponding eigenvalues are given by

$$\lambda_1=-r_P,\quad \lambda_2=r_A+\frac{\epsilon a r_P}{s_P+ahr_P}.$$

Therefore, the plant-only equilibrium E_{P0} is locally stable if $r_A<-\frac{\epsilon a r_P}{s_P+ahr_P}$, while if $r_A>-\frac{\epsilon a r_P}{s_P+ahr_P}$, the plant-only equilibrium E_{P0} is unstable.

(3) *Stability of the animal-only equilibrium* E_{0A}. The Jacobian matrix at E_{0A} can be shown as

$$J(E_{0A})=\begin{pmatrix} r_P+\frac{b_P f\gamma a r_A}{s_A+ar_A} & 0 \\ \frac{r_A}{s_A}\epsilon a & -r_A \end{pmatrix}.$$

Therefore, we have $\lambda_1=r_P+\frac{b_P f\gamma a r_A}{s_A+ar_A}$ and $\lambda_2=-r_A$. That is, the animal-only equilibrium E_{0A} is locally stable if $r_P<-\frac{b_P f\gamma a r_A}{s_A+ar_A}$, while it is unstable if $r_P>-\frac{b_P f\gamma a r_A}{s_A+ar_A}$. This completes the proof of Theorem 3.2. ∎

Appendix B. Proof of Theorem 3.3.

Proof. Assume that $E^* = (P^*, A^*)$ is a coexistence equilibrium of model (2.1); then we have $h_i(P^*, A^*) = 0$, $i = 1, 2$. Solving $h_2(P^*, A^*) = 0$, we obtain

$$A^* = \frac{1}{s_A}\left(r_A + \epsilon \frac{aP^*}{1 + ahP^*}\right). \tag{B.1}$$

Substituting (B.1) into $h_1(P^*, A^*) = 0$ gives

$$H(P^*) := \frac{P^*}{s_A(1+ahP^*)^2 + ar_A(1+ahP^*) + \epsilon aP^*} \cdot H_0(P^*) = 0, \tag{B.2}$$

where

$$\begin{aligned} H_0(P) = &-s_P s_A a^2 h^2 P^3 + \left[s_A r_P a^2 h^2 - 2 s_A a h s_P - s_P a^2 (r_A h + \epsilon)\right] P^2 \\ &+ \left[2 s_A a h r_P + r_P a^2 (r_A h + \epsilon) + b_P f r a^2 (r_A h + \epsilon) - s_A s_P - s_P a r_A\right] P \\ &+ s_A r_P + r_P r_A a + r_A b_P f \gamma a. \end{aligned} \tag{B.3}$$

From the property of cubic equations, we know that the function $H_0(P)$ can have at most two positive real roots if $s_A r_P + r_P r_A a + r_A b_P f \gamma a < 0$ (see Figures 6(a)–(b)), while if $s_A r_P + r_P r_A a + r_A b_P f \gamma a > 0$, the function $H_0(P)$ can have up to three positive real roots (see Figures 6(c)–(d)). Therefore, model (2.1) can have up to three coexistence equilibria if $s_A r_P + r_P r_A a + r_A b_P f \gamma a > 0$, while if $s_A r_P + r_P r_A a + r_A b_P f \gamma a < 0$, model (2.1) has at most two coexistence equilibria.

Next, we verify the stability of the coexistence equilibrium $E^* = (P^*, A^*)$ when it exists. The Jacobian matrix of model (2.1) evaluated at $E^* = (P^*, A^*)$ is

$$J(E^*) = \begin{pmatrix} -P^*\left[\frac{b_P f \gamma a^2 h A^*}{(1+ahP^*+aA^*)^2} + s_P\right] & \frac{b_P f \gamma a P^* (1+ahP^*)}{(1+ahP^*+aA^*)^2} \\ \frac{\epsilon a A^*}{(1+ahP^*)^2} & -s_A A^* \end{pmatrix}.$$

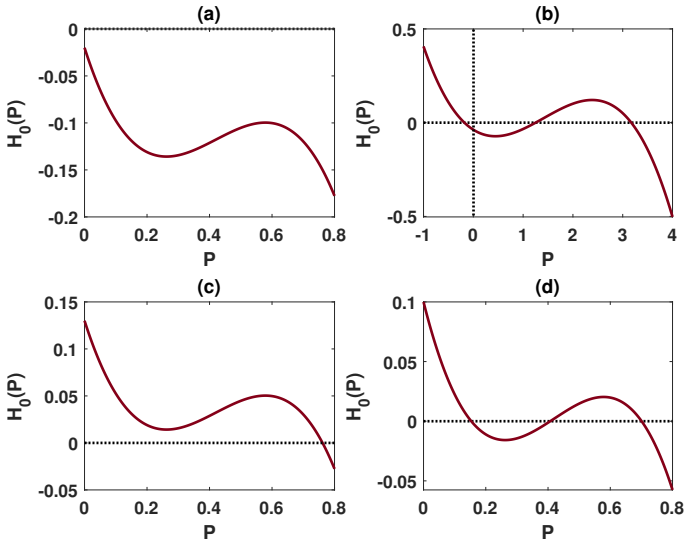

FIG. 6. *Schematic diagram of the function $H_0(P)$. In Figures* 6(a) *and* (b)*, the coefficients satisfy $s_A r_P + r_P r_A a + r_A b_P f \gamma a < 0$, and the function $H_0(P) = 0$ has at most two positive real roots. In Figures* 6(c) *and* (d)*, the coefficients satisfy $s_A r_P + r_P r_A a + r_A b_P f \gamma a > 0$, and the function $H_0(P) = 0$ can have up to three positive real roots.*

The corresponding characteristic equation is given by

$$\lambda^2 + \left[P^*\left(\frac{b_P f\gamma a^2 hA^*}{(1+ahP^*+aA^*)^2} + s_P\right) + s_A A^*\right]\lambda + \det(J(E^*)) = 0, \tag{B.4}$$

where

$$\begin{aligned}\det(J(E^*)) = &\left(\frac{b_P f\gamma a^2 hA^*}{(1+ahP^*+aA^*)^2} + s_P\right) s_A A^* P^* \\ &- \frac{b_P f\gamma a P^*(1+ahP^*)}{(1+ahP^*+aA^*)^2}\frac{\epsilon a A^*}{(1+ahP^*)^2}.\end{aligned}$$

Since $E^* = (P^*, A^*)$ is a coexistence equilibrium of model (2.1), the implicit function theorem combined with $h_2(P^*, A^*) = 0$ implies that there is a continuous differentiable function

$$A(P) = \frac{1}{s_A}\left(r_A + \epsilon\frac{aP}{1+ahP}\right) \tag{B.5}$$

such that $A(P^*) = 0$ and

$$\left.\frac{dA(P)}{dP}\right|_{P=P^*} = -\left.\frac{\frac{\partial h_2(P,A)}{\partial P}}{\frac{\partial h_2(P,A)}{\partial A}}\right|_{P=P^*}.$$

Substituting (B.5) into $h_1(P, A)$, we obtain that

$$h_1(P, A(P)) = H(P). \tag{B.6}$$

Taking the derivative of (B.6) with respect to P, we get that

$$\left[\frac{\partial h_1(P,A(P))}{\partial A}\frac{dA(P)}{dP} + \frac{\partial h_1(P,A(P))}{\partial P}\right]\Bigg|_{P=P^*} = \left.\frac{dH(P)}{dP}\right|_{P=P^*}. \tag{B.7}$$

Therefore, we have

$$\begin{aligned}\left.\frac{dH(P)}{dP}\right|_{P=P^*}\left.\frac{\partial h_2(P,A)}{\partial A}\right|_{P=P^*} &= -\frac{\partial h_1(P,A(P))}{\partial A}\left.\frac{\partial h_2(P,A)}{\partial P}\right|_{P=P^*} \\ &\quad + \left.\frac{\partial h_1(P,A(P))}{\partial P}\right|_{P=P^*}\left.\frac{\partial h_2(P,A)}{\partial A}\right|_{P=P^*} \\ &= \det(J(E^*)).\end{aligned} \tag{B.8}$$

It follows that

$$\begin{aligned}\det(J(E^*)) &= \left.\frac{dH(P)}{dP}\right|_{P=P^*}\left.\frac{\partial h_2(P,A)}{\partial A}\right|_{P=P^*} \\ &= -\frac{s_A A^* P^*}{s_A(1+ahP^*)^2 + ar_A(1+ahP^*) + \epsilon aP^*}\cdot H_0'(P^*).\end{aligned} \tag{B.9}$$

By the characteristic equation (B.4) we know that the eigenvalues satisfy

$$\lambda_1(E^*) + \lambda_2(E^*) = -\left[P^*\left(\frac{b_P f\gamma a^2 hA^*}{(1+ahP^*+aA^*)^2} + s_P\right) + s_A A^*\right] < 0$$

and

$$\lambda_1(E^*)\lambda_2(E^*) = \det(J(E^*)) = -\frac{s_A A^* P^*}{s_A(1+ahP^*)^2 + ar_A(1+ahP^*) + \epsilon aP^*} \cdot H_0(P^*).$$

Therefore, we have Sgn$[\lambda_1(E^*)\lambda_2(E^*)]$ = -Sgn$[H_0'(P^*)]$, i.e., the local stability of a coexistence equilibrium is completely determined by the slope of the cubic equation $H_0(P)$ at this coexistence equilibrium. The remainder of the proof of the local stability is straightforward and therefore omitted here. ∎

Appendix C. Proof of Theorem 3.5.

Proof. Note that model (2.2) satisfies the local Lipschitz condition, and there is a unique local positive solution $(P(t), A(t))$ on $t \in [0, \tau_e)$, where τ_e is the explosion time. If $\tau_e = \infty$, then model (2.2) has a unique global positive solution. To proceed, define n_0 large enough such that $(P(0), A(0)) \in [n_0^{-1}, n_0] \times [n_0^{-1}, n_0]$. For any integer $n \geq n_0$, define the stopping time

$$\tau_n = \inf\{t \in [0, \tau_e) : \min\{P(t), A(t)\} \leq \frac{1}{n} \text{ or } \max\{P(t), A(t)\} \geq n\}.$$

Without loss of generality, define $\inf \emptyset = \infty$. Therefore, we have $\tau_n \uparrow$ as $n \to \infty$. Since $\tau_\infty := \lim_{n\to\infty} \tau_n \leq \tau_e$, model (2.2) has a unique global positive solution if $\tau_\infty = \infty$. Otherwise (i.e., $\tau_\infty < \infty$), there are constants N and $\varepsilon \in (0,1)$ such that $\mathbb{P}\{\tau_\infty \leq N\} > \varepsilon$. That is, we can find an integer $n_1 \geq n_0$ such that

$$\mathbb{P}\{\tau_n \leq N\} > \varepsilon \forall n \geq n_1. \tag{C.1}$$

To continue, we define the Lyapunov function V as

$$V = \int_1^P \frac{s-1}{s} ds + \int_1^A \frac{s-1}{s} ds.$$

Applying Itô's formula to V yields

$$dV = \mathcal{L}V dt + \sigma_1(P-1)dB_1(t) + \sigma_2(A-1)dB_2(t), \tag{C.2}$$

where

$$\begin{aligned}
\mathcal{L}V &= (P-1)\left[b_P f\left(g + \gamma\frac{aA}{1+ahP+aA}\right) - s_P P - d_P\right] + \frac{1}{2}\sigma_1^2 \\
&\quad + (A-1)\left[b_A + \epsilon\frac{aP}{1+ahP} - s_A A - d_A\right] + \frac{1}{2}\sigma_2^2 \\
&\leq (P-1)\left[b_P f g - s_P P - d_P\right] + b_P f\gamma P + \frac{1}{2}\sigma_1^2 \\
&\quad + (A-1)\left[b_A - s_A A - d_A\right] + \frac{\epsilon}{h}A + \frac{1}{2}\sigma_2^2 \\
&\leq -b_P f g + d_P + \frac{1}{2}\sigma_1^2 + \frac{(b_P f g - d_P + s_P + b_P f\gamma)^2}{4s_P} \\
&\quad - b_A + d_A + \frac{1}{2}\sigma_2^2 + \frac{(b_A - d_A + s_A + \frac{\epsilon}{h})^2}{4s_A} := C_0 < \infty.
\end{aligned}$$

Integrating both sides of (C.2) on interval $[0, \tau_n \wedge N]$ yields

$$\mathbb{E}V[P(N\wedge\tau_n), A(N\wedge\tau_n)] \leq V(P(0), A(0)) + C_0 N,$$

where $\mathbb{E}$ represents the mathematical expectation. Define $\Omega_n = \{\tau_n \le N\} \forall n \ge n_1$. By (C.1), we know that $\mathbb{P}(\Omega_n) \ge \varepsilon$. It follows that, for any $\omega \in \Omega_n$, there exists at least one of $P(\tau_n,\omega)$ and $A(\tau_n,\omega)$ that equals either n or n^{-1}. Therefore, we get

$$V(P(\tau_n,\omega),A(\tau_n,\omega)) \ge (n-1-\ln n) \wedge (n^{-1}-1-\ln n^{-1}). \tag{C.3}$$

By (C.2) and (C.3), we have

$$\begin{aligned} V(P(0),A(0)) + C_0 N &\ge \mathbb{E}[\mathbf{1}_{\Omega_n(\omega)} V(P(\tau_n,\omega),A(\tau_n,\omega))] \\ &\ge \varepsilon[(n-1-\ln n) \wedge (n^{-1}-1-\ln n^{-1})], \end{aligned}$$

where $\mathbf{1}_{\Omega_n}$ is the indicator function of Ω_n. Letting $n \to \infty$, we obtain the contradiction that

$$\infty > V(P(0),A(0)) + C_0 N \ge \infty,$$

which indicates that $\tau_\infty = \infty$. This completes the proof of Theorem 3.5. ∎

Appendix D. Proof of Theorem 3.6.

Proof. Define $V(P,A) = P^\theta + A^\theta$, where $\theta \in (0,1)$ is a constant. Applying Itô's formula to $V(P,A)$, we obtain that

$$dV(P,A) = \mathcal{L}V(P,A)dt + \theta\sigma_1 P^\theta dB_1(t) + \theta\sigma_2 A^\theta dB_2(t), \tag{D.1}$$

where

$$\begin{aligned} \mathcal{L}V(P,A) &= \theta P^\theta \left[b_P f\left(g + \gamma \frac{aA}{1+ahP+aA}\right) - s_P P - d_P \right] - \frac{1}{2}\theta(1-\theta)\sigma_1^2 P^\theta \\ &\quad + \theta A^\theta \left[b_A + \epsilon \frac{aP}{1+ahP} - s_A A - d_A \right] - \frac{1}{2}\theta(1-\theta)\sigma_2^2 A^\theta \\ &\le \theta P^\theta \left(b_P f g + b_P f \gamma - d_P - \frac{1}{2}(1-\theta)\sigma_1^2 \right) + P^\theta - s_P \theta P^{\theta+1} \\ &\quad + \theta A^\theta \left(b_A + \frac{\epsilon}{h} - d_A - \frac{1}{2}(1-\theta)\sigma_2^2 \right) - A^\theta - s_A \theta A^{\theta+1} - V(P,A) \\ &\le M - V(P,A), \end{aligned} \tag{D.2}$$

where $M > 0$ is a sufficiently large constant.

Applying Itô's formula to $e^t V(P,A)$ yields

$$\begin{aligned} d[e^t V(P,A)] &= e^t [V(P,A) + dV(P,A)]\, dt + e^t \theta \left(\sigma_1 P^\theta dB_1(t) + \sigma_2 A^\theta dB_2(t)\right) \\ &\le e^t M dt + e^t \theta \left(\sigma_1 P^\theta dB_1(t) + \sigma_2 A^\theta dB_2(t)\right). \end{aligned} \tag{D.3}$$

Choose $n_0 > 0$ such that $(P(0),A(0)) \in [1/n_0, n_0] \times [1/n_0, n_0]$. For any integer $n \ge n_0$, we define the stopping time

$$\tau_n = \inf\{t \in \mathbb{R}_+ : (P(t),A(t)) \in [1/n,n] \times [1/n,n]\}.$$

Integrating both sides of (D.3) from 0 to $t \wedge \tau_n$, we get

$$\mathbb{E}[e^{t\wedge\tau_n} V(P(t\wedge\tau_n), A(t\wedge\tau_n))] - V(P(0),A(0)) \le \mathbb{E}\int_0^{t\wedge\tau_n} e^s M ds. \tag{D.4}$$

Letting $n \to \infty$, it then follows from (D.4) that

$$e^t \mathbb{E}[V(P(t), A(t))] \leq V(P(0), A(0)) + (e^t - 1)M,$$

which indicates that

$$\limsup_{t \to \infty} \mathbb{E}[V(P(t), A(t))] \leq M. \tag{D.5}$$

The expected result is straightforward by applying Chebyshev's inequality to (D.5). ∎

REFERENCES

[1] R. Arumugam, F. Lutscher, and F. Guichard, *Tracking unstable states: Ecosystem dynamics in a changing world*, Oikos, 130 (2021), pp. 525–540.

[2] C. E. Aslan, E. S. Zavaleta, B. Tershy, and D. Croll, *Mutualism disruption threatens global plant biodiversity: A systematic review*, PLoS One, 8 (2013), e66993.

[3] J. Bascompte, P. Jordano, and J. M. Olesen, *Asymmetric coevolutionary networks facilitate biodiversity maintenance*, Science, 312 (2006), pp. 431–433.

[4] I. Bashkirtseva, T. Ryazanova, and L. Ryashko, *Confidence domains in the analysis of noise-induced transition to chaos for Goodwin model of business cycles*, Internat. J. Bifur. Chaos Appl. Sci. Engrg., 24 (2014), 1440020.

[5] R. Benzi, A. Sutera, and A. Vulpiani, *The mechanism of stochastic resonance*, J. Phys. A, 14 (1981), pp. 453–457.

[6] H. C. Bumpus, *The Elimination of the Unfit as Illustrated by the Introduced Sparrow, Passer Domesticus (A Fourth Contribution to the Study of Variation)*, Gin, 1899.

[7] L. G. Carvalheiro, I. Bartomeus, O. Rollin, S. Timóteo, and C. F. Tinoco, *The role of soils on pollination and seed dispersal*, Philos. Trans. Roy. Soc. B, 376 (2021), 20200171.

[8] L. Dai, D. Vorselen, K. S. Korolev, and J. Gore, *Generic indicators for loss of resilience before a tipping point leading to population collapse*, Science, 336 (2012), pp. 1175–1177.

[9] P. D. Ditlevsen and S. J. Johnsen, *Tipping points: Early warning and wishful thinking*, Geophys. Res. Lett., 37 (2010), L19703.

[10] C. I. Donatti, P. R. Guimarães, M. Galetti, M. A. Pizo, F. M. Marquitti, and R. Dirzo, *Analysis of a hyper-diverse seed dispersal network: Modularity and underlying mechanisms*, Ecol. Lett., 14 (2011), pp. 773–781.

[11] S. P. Ellner and M. Rees, *Stochastic stable population growth in integral projection models: Theory and application*, J. Math. Biol., 54 (2007), pp. 227–256.

[12] T. Feng, D. Charbonneau, Z. Qiu, and Y. Kang, *Dynamics of task allocation in social insect colonies: Scaling effects of colony size versus work activities*, J. Math. Biol., 82 (2021), 42.

[13] T. Feng, R. Milne, and H. Wang, *Variation in environmental stochasticity dramatically affects viability and extinction time in a predator–prey system with high prey group cohesion*, Math. Biosci., 365 (2023), 109075.

[14] T. Feng, Z. Qiu, and Y. Kang, *Recruitment dynamics of social insect colonies*, SIAM J. Appl. Math., 81 (2021), pp. 1579–1599, https://doi.org/10.1137/20M1332384.

[15] T. Feng, H. Zhou, Z. Qiu, and Y. Kang, *Impacts of demographic and environmental stochasticity on population dynamics with cooperative effects*, Math. Biosci., 353 (2022), 108910.

[16] G. F. Gause and A. Witt, *Behavior of mixed populations and the problem of natural selection*, Amer. Nat., 69 (1935), pp. 596–609.

[17] A. Gray, D. Greenhalgh, L. Hu, X. Mao, and J. Pan, *A stochastic differential equation SIS epidemic model*, SIAM J. Appl. Math., 71 (2011), pp. 876–902, https://doi.org/10.1137/10081856X.

[18] J. Guckenheimer and P. Holmes, *Nonlinear Oscillations, Dynamical Systems, and Bifurcations of Vector Fields*, Appl. Math. Sci. 42, Springer-Verlag, New York, 2013.

[19] K. R. Hale, D. P. Maes, and F. S. Valdovinos, *Simple mechanisms of plant reproductive benefits yield different dynamics in pollination and seed dispersal mutualisms*, Amer. Nat., 200 (2022), pp. 202–216.

[20] K. R. Hale and F. S. Valdovinos, *Ecological theory of mutualism: Robust patterns of stability and thresholds in two-species population models*, Ecol. Evol., 11 (2021), pp. 17651–17671.

[21] A. Hening and D. H. Nguyen, *Coexistence and extinction for stochastic Kolmogorov systems*, Ann. Appl. Probab., 28 (2018), pp. 1893–1942.
[22] D. J. Higham, *An algorithmic introduction to numerical simulation of stochastic differential equations*, SIAM Rev., 43 (2001), pp. 525–546, https://doi.org/10.1137/S0036144500378302.
[23] J. N. Holland and D. L. DeAngelis, *A consumer–resource approach to the density-dependent population dynamics of mutualism*, Ecology, 91 (2010), pp. 1286–1295.
[24] T. P. Hughes, J. T. Kerry, A. H. Baird, S. R. Connolly, A. Dietzel, C. M. Eakin, S. F. Heron, A. S. Hoey, M. O. Hoogenboom, G. Liu, M. J. McWilliam, R. J. Pears, M. S. Pratchett, W. J. Skirving, J. S. Stella, and G. Torda, *Global warming transforms coral reef assemblages*, Nature, 556 (2018), pp. 492–496.
[25] L. Imhof and S. Walcher, *Exclusion and persistence in deterministic and stochastic chemostat models*, J. Differential Equations, 217 (2005), pp. 26–53.
[26] R. A. Ims, J.-A. Henden, and S. T. Killengreen, *Collapsing population cycles*, Trends Ecol. Evol., 23 (2008), pp. 79–86.
[27] C. A. Johnson and P. Amarasekare, *Competition for benefits can promote the persistence of mutualistic interactions*, J. Theoret. Biol., 328 (2013), pp. 54–64.
[28] T. Latty and V. Dakos, *The risk of threshold responses, tipping points, and cascading failures in pollination systems*, Biodivers. Conserv., 28 (2019), pp. 3389–3406.
[29] D. Lee and M. Strauss, *Giraffe demography and population ecology*, in Reference Module in Earth Systems and Environmental Sciences, Elsevier, Amsterdam, 2016, pp. 1–9.
[30] X. Mao, *Stationary distribution of stochastic population systems*, Systems Control Lett., 60 (2011), pp. 398–405.
[31] R. Medel, C. Botto-Mahan, and M. Kalin-Arroyo, *Pollinator-mediated selection on the nectar guide phenotype in the Andean monkey flower, mimulus luteus*, Ecology, 84 (2003), pp. 1721–1732.
[32] Y. Meng, Y.-C. Lai, and C. Grebogi, *Tipping point and noise-induced transients in ecological networks*, J. R. Soc. Interface, 17 (2020), 20200645.
[33] T. Okuyama and J. N. Holland, *Network structural properties mediate the stability of mutualistic communities*, Ecol. Lett., 11 (2008), pp. 208–216.
[34] J. Oliveira, A. Destro, M. Freitas, and L. Oliveira, *How do pesticides affect bats?–a brief review of recent publications*, Braz. J. Biol., 81 (2020), pp. 499–507.
[35] E. Post, M. C. Forchhammer, M. S. Bret-Harte, T. V. Callaghan, T. R. Christensen, B. Elberling, A. D. Fox, O. Gilg, D. S. Hik, T. T. Høye, R. A. Ims, E. Jeppesen, D. R. Klein, J. Madsen, A. D. McGuire, S. Rysgaard, D. E. Schindler, I. Stirling, M. P. Tamstorf, N. J. C. Tyler, R. van der Wal, J. Welker, P. A. Wookey, N. M. Schmidt, and P. Aastrup, *Ecological dynamics across the Arctic associated with recent climate change*, Science, 325 (2009), pp. 1355–1358.
[36] T. A. Revilla, *Numerical responses in resource-based mutualisms: A time scale approach*, J. Theoret. Biol., 378 (2015), pp. 39–46.
[37] R. S. Robeva, *Algebraic and Discrete Mathematical Methods for Modern Biology*, Academic Press, New York, 2015.
[38] L. Ryashko, *Sensitivity analysis of the noise-induced oscillatory multistability in Higgins model of glycolysis*, Chaos, 28 (2018), 033602.
[39] L. P. Sales, W. D. Kissling, M. Galetti, B. Naimi, and M. M. Pires, *Climate change reshapes the eco-evolutionary dynamics of a neotropical seed dispersal system*, Glob. Ecol. Biogeogr., 30 (2021), pp. 1129–1138.
[40] M. Sankaran, N. P. Hanan, R. J. Scholes, J. Ratnam, D. J. Augustine, B. S. Cade, J. Gignoux, S. I. Higgins, X. Le Roux, F. Ludwig, J. Ardo, F. Banyikwa, A. Bronn, G. Bucini, K. K. Caylor, M. B. Coughenour, A. Diouf, W. Ekaya, C. J. Feral, E. C. February, P. G. H. Frost, P. Hiernaux, H. Hrabar, K. L. Metzger, H. H. T. Prins, S. Ringrose, W. Sea, J. Tews, J. Worden, and N. Zambatis, *Determinants of woody cover in African savannas*, Nature, 438 (2005), pp. 846–849.
[41] M. Scheffer, S. Carpenter, J. A. Foley, C. Folke, and B. Walker, *Catastrophic shifts in ecosystems*, Nature, 413 (2001), pp. 591–596.
[42] M. Scheffer and R. J. De Boer, *Implications of spatial heterogeneity for the paradox of enrichment*, Ecology, 76 (1995), pp. 2270–2277.
[43] F. Seebacher and E. Post, *Climate change impacts on animal migration*, Climate Change Responses, 2 (2015), pp. 1–2.
[44] B. H. Tiffney and S. J. Mazer, *Angiosperm growth habit, dispersal and diversification reconsidered*, Evol. Ecol., 9 (1995), pp. 93–117.

[45] F. S. Valdovinos, P. Moisset de Espanés, J. D. Flores, and R. Ramos-Jiliberto, *Adaptive foraging allows the maintenance of biodiversity of pollination networks*, Oikos, 122 (2013), pp. 907–917.
[46] J. H. Vandermeer and D. H. Boucher, *Varieties of mutualistic interaction in population models*, J. Theoret. Biol., 74 (1978), pp. 549–558.
[47] Y. Zhou, C. Newman, J. Chen, Z. Xie, and D. W. Macdonald, *Anomalous, extreme weather disrupts obligate seed dispersal mutualism: Snow in a subtropical forest ecosystem*, Glob. Change Biol., 19 (2013), pp. 2867–2877.